Knitted Fabrics with Dyneema® Fibres for Ballistic Protection: Modelling and Experimental Validation of a Single Jersey Knit

M. Hazzard[1], U. Heisserer[1], M. van der Kamp[1], K. Freier[1]

[1]DSM Protective Materials, Urmonderbaan 22, 6167 Geleen, The Netherlands
mark.hazzard@dsm.com

Abstract. High strength UHMWPE fibres and their composites have been widely used in personal protection due to their excellent tensile strength and low weight. Typically, this protection is in the form of a hard or a soft ballistic panel of cross-ply unidirectional sheets which cover critical body parts, with protection level often requiring a balance between mobility and resistance. Knits based on UHMWPE provide the opportunity for increased personal protection by increasing the protection level on difficult to cover areas requiring high mobility and drapability. Knits intrinsically allow for more extensibility compared with weaves or cross-ply unidirectional sheets by making use of yarn curvature, something that is intrinsic to the yarn path geometry of a knit. Here, a simplistic finite element modelling approach has been used with tensile only beam elements to capture the behaviour of UHMWPE knits, branded as Dyneema®, in a ballistic setting with a single jersey knit architecture. The behaviour of the single jersey knit has been compared to performance of other form factors with experimental data and readily available data from literature, which highlights the potential of UHMWPE frag protective knits.

1. INTRODUCTION

UHMWPE fibre based personal protection, such as Dyneema® UD, has been offered in technology platforms such as soft ballistic sheets and hard ballistic panels for excellent lightweight protection due to the fibres intrinsic low weight and high tenacity [1]. The UD form factor is extremely well suited for ballistic performance as fibres are straight with no yarn cross-overs, providing minimal back face deformation and excellent ballistic limit. However, in order to increase the level of personal protection, form factors should be considered that cover areas of the body that require higher mobility/drapability. Knits are typically the go to form factor for comfort and are used for clothing and apparel in commodity textiles. Knits allow for extensibility through incorporation of yarn curvature, and without a binder system, are highly extensible and drapable. For high performance UHMWPE yarns that are intrinsically stiff in tension, comfort and extensibility can therefore be provided by exploiting hidden length within the knit geometry. This combines to allow for greater stretch, flexibility, and shear, providing increased comfort for those hard to cover areas of the body.

The simplest and most common type of knit is the single jersey knit comprising courses (loops side by side) and wales (interlocking of those loops vertically). Dwivedi *et al* [2], [3] compared multiple types of fabrics including felts, weaves, and knits through mechanical testing followed by ballistic trials. They showed that continuous filament knits with a high performance yarn provide a unique combination of extensibility and perforation levels. Aramid weaves, for example, provided an initial elastic modulus 4 orders of magnitude higher than a comparable aramid knit, yet the ballistic performance for a similar areal density knit was only reduced by 10-15% [3]. Architecture can therefore play a role in both ballistic performance and comfort levels, however for a given architecture, the intrinsic yarn properties are still expected to be a governing factor. Using the Cunniff parameter, a combination of specific tenacity and tensile wave speed of the fiber [4], Werff *et al* [5] highlights the potential of UHMWPE fibres in terms of ballistic performance due to their high tenacity, low density, and high modulus. This paper aims to show the performance of a continuous filament single jersey knit structure made with Dyneema® through an experimental approach. Using this data, a simplistic numerical modelling approach is outlined that is validated with this experimental data. The finite element modelling approach allows further investigation into the drivers of performance for knits for ballistic protection, with an example comparison to an aramid yarn provided.

https://doi.org/10.52202/078352-0005

2. METHODOLOGY

2.1 Experimental

Single jersey knits were produced using a flatbed Shima Seiki with a Dyneema® 880 dtex yarn. Following knitting, 10 samples were cut to approximately 200×200 mm square patch, and to give some rigidity for handling, the sample was edged with duct tape. For ballistic testing, the sample was held to the frame with a small piece of duct tape to maintain its position, allowing numerical models to be considered free of boundary conditions. A 1.1 g fragment simulating projectile (FSP) was used, impacting approximately central to the target with a single shot. Velocity light gates were positioned in front and behind the target to capture an initial velocity (V_I) and a residual velocity (V_R) for the samples that were perforated. A ballistic limit was then estimated using a Lambert-Jonas approximation [6]. Additionally, a Photron fastcam SA5 was used to record the impact event with two illuminating Dedolight 400D lights. The camera was positioned at an angle of approximately 30° from the side on view of the knit in order to estimate the back face deformation whilst also have capability to measure wave propagation rates within the knit. Reference images were taken with reference geometry to extract absolute geometry and the precise angle of the camera relative to the sample. 3D position cannot be extracted with a single camera, hence the assumption was that wave propagation happens only in X and Y directions (in plane), whilst maximum back face deformation only in the Z direction (out of plane). The full setup is given in Figure 1. ImageJ was used to extract both the back face deformation with time as well as the shock wave velocity within the knit.

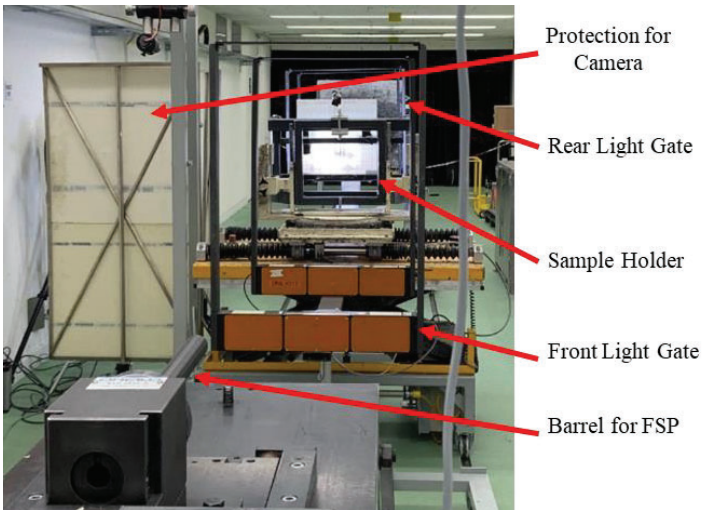

Figure 1: Image of ballistic setup.

2.2 Numerical

Recently, McKee *et al* [7] outlined a modelling method to first capture the geometry of a single jersey knit and meshing with a solid elements (Figure 2) using a transversely isotropic constitutive model for material behaviour to simulate ballistic impact. This provided reasonable correlation to experimental results in terms of wave propagation and back face deformation. One difficulty, particularly when capturing failure of yarns through a continuum approach, is the difficulty in homogenizing discontinuous filaments in a yarn, and the effects this has upon failure.

https://doi.org/10.52202/078352-0005

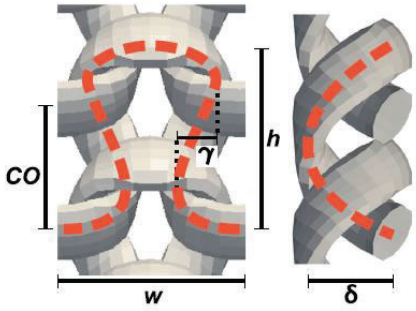

$$x(s) = \frac{s}{\lambda}w + \gamma \sin\left(4\pi\frac{s}{\lambda}\right) \quad (1)$$

$$y(s) = CO + \frac{h}{2}\cos\left(2\pi\frac{s}{\lambda}\right) \quad (2)$$

$$z(s) = \frac{\delta}{2}\cos\left(4\pi\frac{s}{\lambda}\right) \quad (3)$$

Figure 2: McKee *et al* [7] 3D solid representation, with parameters *CO* course offset, *w* loop width, γ loop curvature length, *h* loop height, δ thickness, and λ loop path length.

Here, we utilized the geometrical parameters outlined by McKee *et al* [7] but implement it using tensile only beam elements with an equivalent circular cross section within LS-DYNA (MAT CABLE DISCRETE BEAM). This model assumes perfect Hookean elasticity, with an UHMWPE modulus of 155 GPa and a density of 0.98 g/cm^3, and as yet, does not incorporate a failure model. This has reduced complexity and does not capture variations in yarn geometry along the loop path or variation in stress across a yarn, however this does allow for minimal run time whilst avoiding difficulties associated with continuum modelling of yarns. Measurements of knit geometry were performed via optical microscopy with the exception of δ (thickness) and λ (loop path length). These parameters can be solved analytically from a known areal density of the system (Table 1) and the yarn dtex. For this 1D approximation, the path length (and areal density) of the knit geometry can be dependent on the number of elements. For example, a coarse mesh has reduced length compared to the natural curvature of the knit that has not be discretised into elements. For the current construction, 20 elements were used per loop. The geometry of the model is provided in Figure 3 with the circular cross section visible, and the geometrical parameters provided in Table 1.

Table 1: Geometrical parameters used for the UHMWPE knit.

Geometrical Parameter	Value	Unit
w	1.9	mm
γ	0.4	mm
CO	0.71	mm
h	1.263	mm
δ	0.54	mm
Yarn	880	dtex
Areal Density	0.34748	(kg/m^2)
No. Elements per loop	20	-

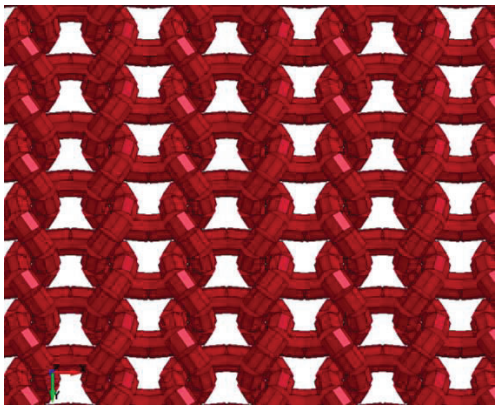

Figure 3: Finite element modelling highlighting circular cross section.

https://doi.org/10.52202/078352-0005

The projectile was modelled using geometry from the standard assuming no end flange [8]. The FSP was meshed with 0.5 mm solid quad-elements with a single integration point (formulation type 1 in LS-DYNA). A simplified Johnson Cook material model was used for the projectile with parameters taken directly from literature [9]. Automatic general contact was applied with SOFT=1 and a coefficient of static and dynamic friction of 0.1 within the model. An additional damping frequency range was utilised in order to damp out non-physical modes of deformation, particularly after initial contact, driven by natural frequencies of beam elements and the repeating unit of the knit structure. Care was taken to select damping frequencies that do not influence the result and induce additional energy loss. A frequency range of 500 to 10000 Hz was applied only to the knitted part with a damping coefficient of 0.1. Lower frequencies of damping, particularly below 500 Hz, were observed to induce faster projectile deceleration, indicating a non-physical energy loss (Figure 4).

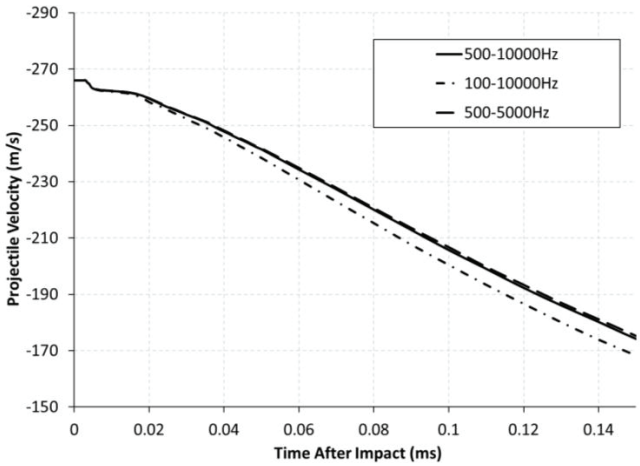

Figure 4: Projectile velocity with time from a 1.1 g FSP impact simulation at 266 m/s whilst varying the frequency damping range.

3. RESULTS

3.1 Experimental Results

Initial and residual velocities from 10 shots with a Lambert-Jonas fit are given in Figure 5, with the Lambert Jonas equation used for fitting also given (eq. 4). In total there were 5 stops and 5 penetrations, which indicate that the ballistic limit (V_{BL}) is approximately 290 m/s with a sharp stop transition for the non-commercial knit. This can be observed through high p values compared to other form factors and velocity ranges which typically have values in the range of 2-4 [10].

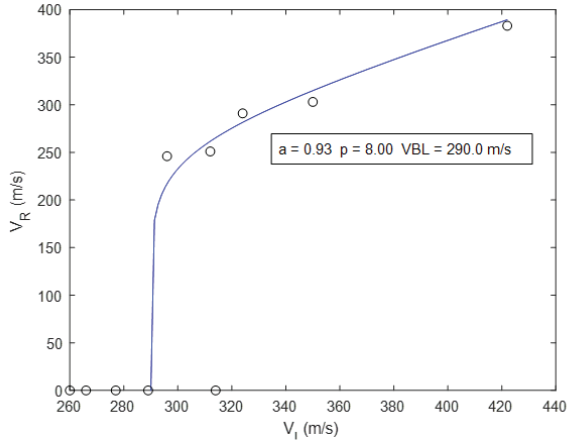

$$V_R = a\left(V_I^p - V_{BL}^p\right)^{1/p} \qquad (4)$$

Figure 5: Initial velocity vs residual velocity of each shot with a Lambert-Jonas fit for ballistic limit. Note that the single jersey knit is non-commercial and does not consider additional requirements for application.

https://doi.org/10.52202/078352-0005

A high speed image sequence of a stop event with an impact velocity of 266 m/s is given in Figure 6. The sample can be observed at t = 0 prior to impact with surrounding duct tape around the sample. The centre of the sample is visualized by marking it with a pen. There was a small variation in impact location, however the location was always within 20 mm of the centre location, whilst the FSP had negligible pitch or yaw. Some waviness in the sample is observed and can be attributed to the low flexural stiffness of knits compared with other form factors whilst the knitting process itself can induce some residual stress following manufacture. After impact, the longitudinal waves (in-plane of the knit) can be observed propagating along the yarns ahead of the shear hinge (out-of-plane of the knit). For comparison to numerical results, the position of the waves in the vertical and horizontal directions have been tracked in each frame, with the location and orientation also highlighted in Figure 5 (P_{LV}, P_{LH}, P_{SV} P_{SH}). Once the longitudinal wave has reached the boundary, pull in of the fabrics can be observed from the edge. Locally around the projectile the knit exhibits additional stretch and opening up of the course and wale structure, where visually the gaps between yarns can become larger. This is shown in Figure 7a with an image taken after the impact event.

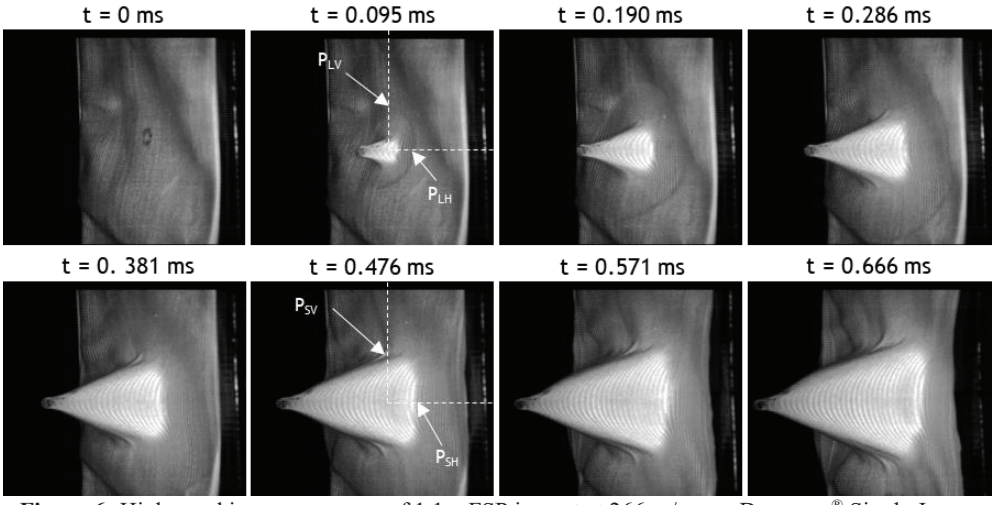

Figure 6: Highspeed image sequence of 1.1 g FSP impact at 266 m/s on a Dyneema® Single Jersey Knit with a stop. Position of measured wave position indicated on image for the Position Longitudinal Vertical wave (P_{LV}), the Position Longitudinal Horizontal wave (P_{LH}), the Position of the Shear-hinge Vertical (P_{SV}), and the Position of the Shear-hinge Horizontal (P_{SH}).

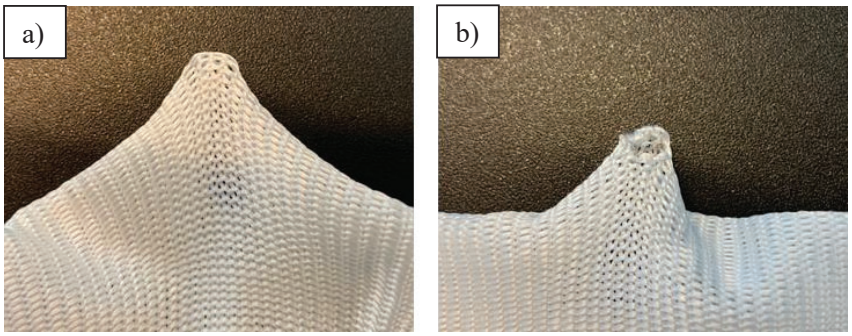

Figure 7: Image following impact of a) 266 m/s stop case, b) 324 m/s penetration case.

A highspeed image sequence is now also given for a penetration case in Figure 8. Its shown that the failure event happens early on in the impact process. A zoom view focusing on the impact location is also shown, and following inspection it appears as though a single yarn has failed which allows opening of the knit. The damage zone of the impact location is also provided in Figure 7b.

https://doi.org/10.52202/078352-0005

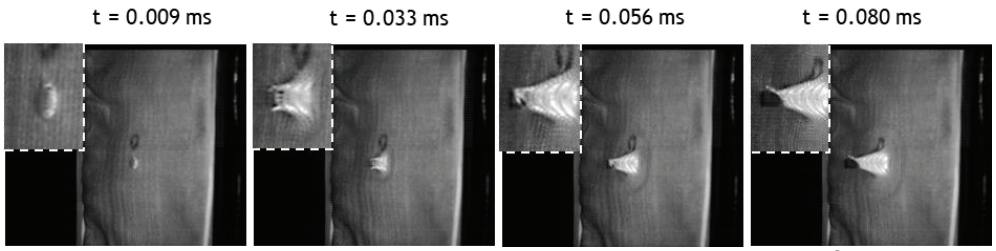

Figure 8: Highspeed image sequence of 1.1 g FSP impact at 324 m/s on a Dyneema® Single Jersey Knit with a penetration. Top left of each images isolates a close up of the impact location.

3.2 Numerical Validation

A stop case of 266 m/s was simulated with an image sequence following impact provided in Figure 9. Within the model, the longitudinal wave can be seen progressing ahead of the shear hinge as back face deformation develops. Maximum back face deformation is compared with that measured experimentally from highspeed images in Figure 10. The simple tensile only beam approach is surprisingly accurate. This seems to suggest that back face deformation is largely driven by conservation of momentum, and if the areal density is matched along with wave speeds, then a reasonable back face deformation can be expected. This also suggests that the low flexural rigidity of the knit provides little resistance to back face deformation, and that changes in back face deformation would be largely momentum driven as well as boundary dependent.

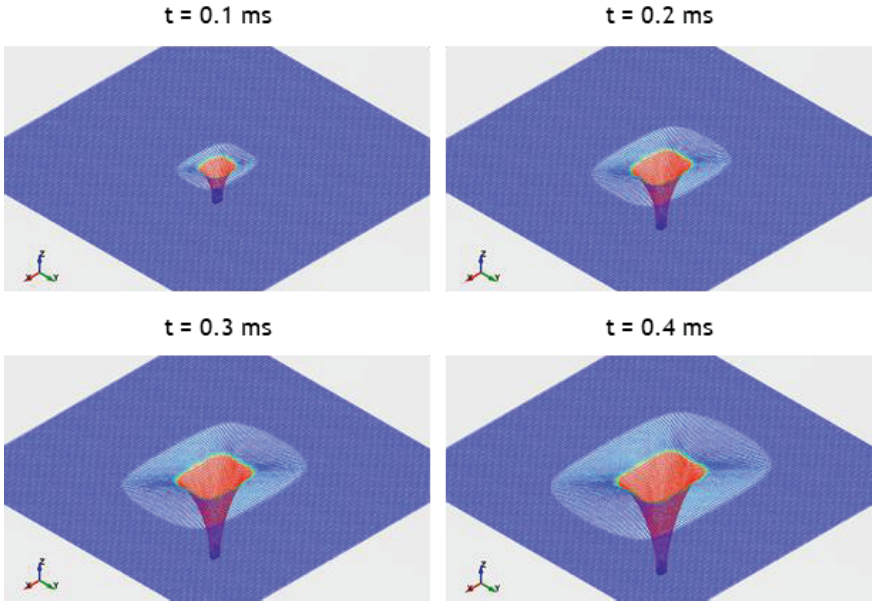

Figure 9: Numerical model image sequence with an isometric view with time after impact, t, indicated above each image. Red indicates more than 1 mm back face deformation, with the transition zone the approximate location of the shear hinge. In this image, the beam elements are visualised in only 1D.

https://doi.org/10.52202/078352-0005

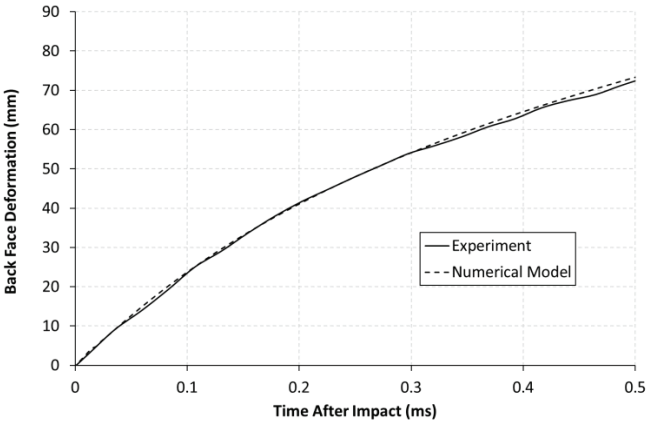

Figure 10: Back face deformation of Dyneema® Single Jersey Knit with a stop at 266 m/s.

Figure 11 compares the wave position for the horizontal and vertical longitudinal and shear waves measured experimentally and numerically. It was observed that longitudinal wave propagation was slower in the model than observed experimentally. This was observed in both the horizontal and vertical direction (Figure 11a and Figure 11b respectively). It is thought that the longitudinal wave speed difference is due to the difference in the simplified geometrical model used compared with that in reality. That being said, the model does capture the higher wave speed in the horizontal compared with the vertical direction. Note that the horizontal direction has a continuous filament as this is the course direction, whilst the vertical direction the wave needs to be transferred via interlocking loops (wales). This indicates that the modelled knit has a similar degree of anisotropy compared with the experimental result.

When considering the shear hinge speed, it was observed that the numerical model was reasonably accurate in both the horizontal and vertical direction until approximately 0.2 ms (Figure 11c-d). After this time, the results start to diverge, with the numerical model again progressing slower. One possible explanation for this is that boundary interaction within the experiment can start to occur due to faster longitudinal wave propagation observed in the experiment. The shot is not perfectly central, and duct tape may start to have an influence after approximately 60 mm travel of the longitudinal wave speed. There may also be some variability in true length to the boundary due to waviness in the knitted sample (observable in Figure 6). Again though, the difference in horizontal and vertical shear wave speed is captured in the simplistic model.

https://doi.org/10.52202/078352-0005

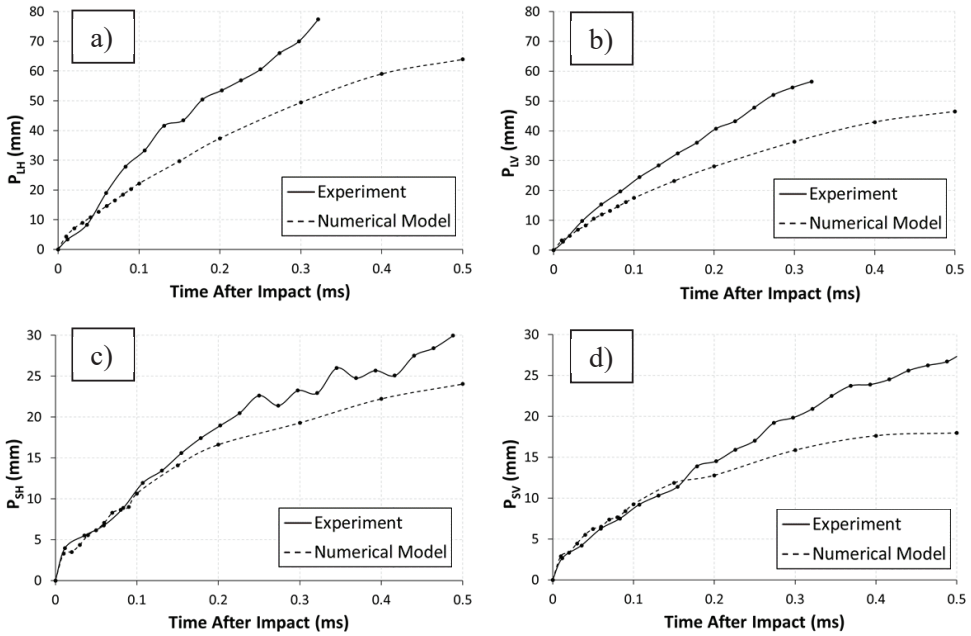

Figure 11: Comparison of wave speeds between experimental results and the numerical model. a) Position Longitudinal Horizontal wave (P_{LH}), b) Position of the Longitudinal Vertical wave (P_{LV}), c) the Position of the Shear-hinge Horizontal (P_{SH}), and d) the Position of the Shear-hinge Vertical (P_{SV}).

3.3 Comparison to Aramid

Numerical modelling allows direct comparison of individual parameters that are often difficult to perform experimentally. As such, a simulation was performed with an aramid yarn at the same dtex. This required a reduction in cross sectional area of the yarn, but the areal density and geometry of the knit are identical. This dictates that the aramid knit intrinsically has a reduction in coverage area, the frontal area of the knit that contains gaps, compared with UHMWPE yarns for the same construction and areal density.

Table 2: Table of yarn properties used for comparison

Parameter	Aramid	UHMWPE	Unit
Density	1.44 [7]	0.98	g/cm^3
Modulus	82.6 [7]	155	GPa
Tensile Strength*	3.88 [11]	4.2	GPa

** Tensile strength not incorporated in the model, only for reference, aramid assumed Kevlar KM2.*

No failure/damage model was incorporated into the numerical modelling approach as tensile only beam elements assume constant stress over the cross sectional area. McKee *et al* [7] using solid elements has shown this is not the case, with stresses varying throughout the yarn from filament to filament. This would suggest that for our model, an equivalent force at failure would need to be defined for each yarn and each geometrical construction. However, we can compare maximum axial force observed in the yarn at a certain moment in time for a certain impact speed. The maximum force of the yarn was observed to vary dependent on the location in the loop and its location relative to the projectile. For this simple comparison, we compare the same element at an approximately central location under the impactor at the top of the loop (Figure 13). It was observed that there is some initial noise which has been assumed to be numerically driven and for the purpose of this comparison was assumed negligible. This is also supported by highspeed imagery, where failure did not occur until a later moment in time (Figure 8, 324 m/s impact example). The forces observed reach a similar maximum magnitude following some initiation noise (location highlighted), and assuming a similar stress distribution across a yarn at that location, then force at failure would largely be strength and cross sectional area dependent.

https://doi.org/10.52202/078352-0005

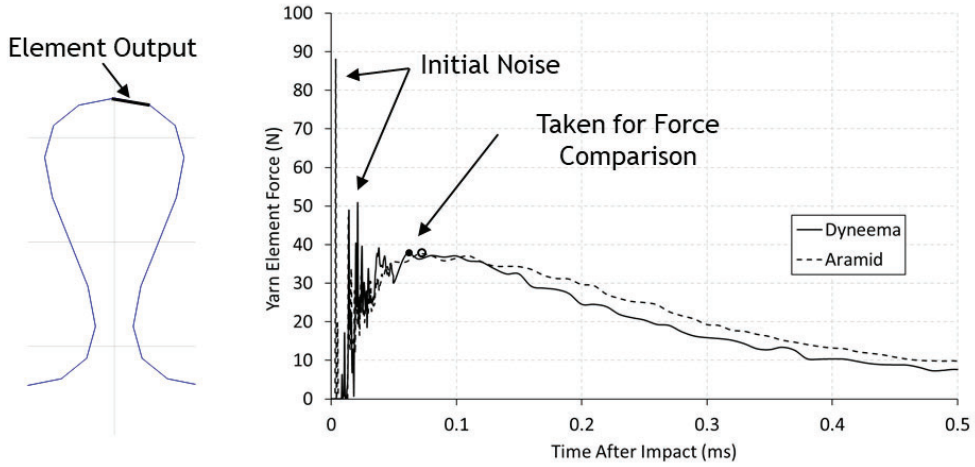

Figure 12: Force comparison within a single element

Whilst this comparison is not perfect as this does not consider several phenomena such as precise location of max force in the knit and variation of force over the yarn cross-section, it does suggest that as the tensile strength and cross-section of the yarn is higher for UHMWPE, on a weight basis, UHMWPE should outperform an aramid. An experimental comparison of V_{50} performance in Figure 13 highlights the potential a Dyneema® Knits. This is done through making use of non-dimensional areal density [4], which is a method to compare ballistic performance where differing projectiles have been used. This method also has its limitations as it is limited to blunt projectiles which themselves have variability in performance, whilst it makes no adjustment for the backing that was utilised (aramid comparisons have gelatin backing whilst here results are free hanging). However, the Dyneema® Single Jersey Knit shown experimentally here has similar ballistic limit to that of an aramid single jersey knit, yet with a drastic reduction in non-dimensional areal density. This also demonstrates that the application of knits compared with other form factors, such as hard ballistic panels (HB26 Dyneema® reference provided [10]), are best at providing protection in a lower areal density range.

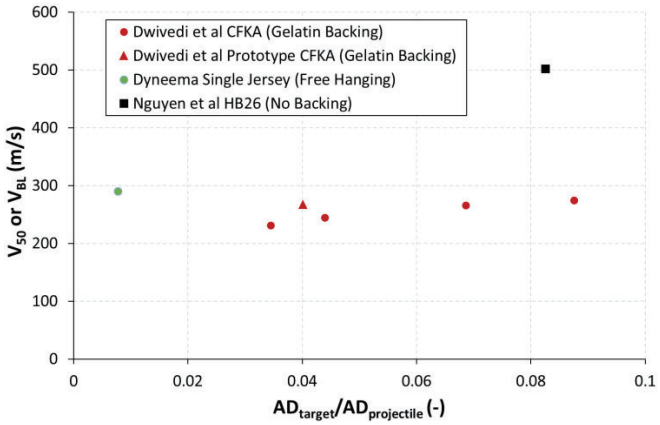

Figure 13: Ballistic performance of non-commercial Dyneema® single jersey knit compared with literature. Note that the single jersey knit is non-commercial and does not consider additional requirements for application.

4. CONCLUSION

This contribution has highlighted the potential of Dyneema® knits as a way to increase personal protection by providing protection for those hard to cover areas requiring high mobility and drapability.

https://doi.org/10.52202/078352-0005

We demonstrate:

- Excellent ballistic performance of a Dyneema® single jersey knit with a low areal density.
- Numerical modelling alongside ballistic experimental results suggest that Dyneema® single jersey knits outperform other knits where data was available in literature.
- Summarising, the form factor of knits for ballistic protection is well suited to those applications at lower areal densities requiring high mobility.

The numerical modelling method provided for investigating the behaviour of knits matched experimental back face deformation well, whilst trends in shock wave propagation were also captured. This type of 1D modelling has fast run times and avoids difficulties in approximating through thickness properties of yarns. As this method does not capture through thickness behaviour, element instabilities of solid elements under large deformations in a dynamic impact environment are also avoided. However, drawbacks include the inability to capture stress variation across the yarn thickness and its contribution to a desirable failure model. As such, a failure model is currently not incorporated.

Acknowledgments

The authors would like to acknowledge the support of Bart Schoonenberg, Mildred Janssens, and Rene Raets for the help in production and testing of single jersey knit fabrics. We would also like to thank Ilse Maes and Pierre Noyrez for their support in imaging and measuring the knitted constructions for details required for numerical modelling input.

References

[1] H. van der Werff and U. Heisserer, "High-performance ballistic fibers: ultra-high molecular weight polyethylene (UHMWPE)," in *Advanced Fibrous Composite Materials for Ballistic Protection*, Woodhead Publishing, 2016, pp. 71–107.

[2] a. Dwivedi *et al.*, "Continuous filament knit aramids for extremity ballistic protection," *28th Annu. Tech. Conf. Am. Soc. Compos. 2013, ASC 2013*, vol. 1, pp. 767–777, 2013.

[3] A. K. Dwivedi, M. W. Dalzell, S. a. Fossey, K. a. Slusarski, L. R. Long, and E. D. Wetzel, "Low velocity ballistic behavior of continuous filament knit aramid," *Int. J. Impact Eng.*, vol. 96, pp. 23–34, 2016.

[4] P. M. Cunniff, "Dimensionless parameters for optimization of textile-based body armor systems," in *Proceedings of the 18th International Symposium on Ballistics*, 1999, pp. 1303–10.

[5] U. Heisserer and H. van der Werff, "The relation between Dyneema® fiber properties and ballistic protection performance of its fiber composites," in *15th International Conference on Deformation, Yield and Fracture of Polymers*, 2012, vol. 3, pp. 242–246.

[6] J. Lambert and G. Jonas, "Towards standardization in terminal ballistics testing: velocity representation," no. Technical report AD-A021 389. Ballistic Research Laboratories Aberdeen Proving Ground, MD, 1976.

[7] P. J. McKee, A. C. Sokolow, J. H. Yu, L. L. Long, and E. D. Wetzel, "Finite element simulation of ballistic impact on single jersey knit fabric," *Compos. Struct.*, vol. 162, pp. 98–107, 2017.

[8] "MIL-DTL-46593B," no. July. 2006.

[9] M. K. Hazzard, R. S. Trask, U. Heisserer, M. Van Der Kamp, and S. R. Hallett, "Finite Element Modelling of Dyneema ® Composites : From Quasi- Static Rates to Ballistic Impact," *Compos. Part A Appl. Sci. Manuf.*, vol. 115, pp. 31–45, 2018.

[10] L. Nguyen, T. Lässig, S. Ryan, and W. Riedel, "A methodology for hydrocode analysis of ultra-high molecular weight polyethylene composite under ballistic impact," *Compos. Part A Appl. Sci. Manuf.*, vol. 84, pp. 224–235, 2016.

[11] M. Cheng, W. Chen, and T. Weerasooriya, "Mechanical properties of Kevlar® KM2 single fiber," *J. Eng. Mater. Technol. Trans. ASME*, vol. 127, no. 2, pp. 197–203, 2005.

https://doi.org/10.52202/078352-0005